iScience

CellPress
OPEN ACCESS

Article

Deficiency of *nde1* in zebrafish induces brain inflammatory responses and autism-like behavior

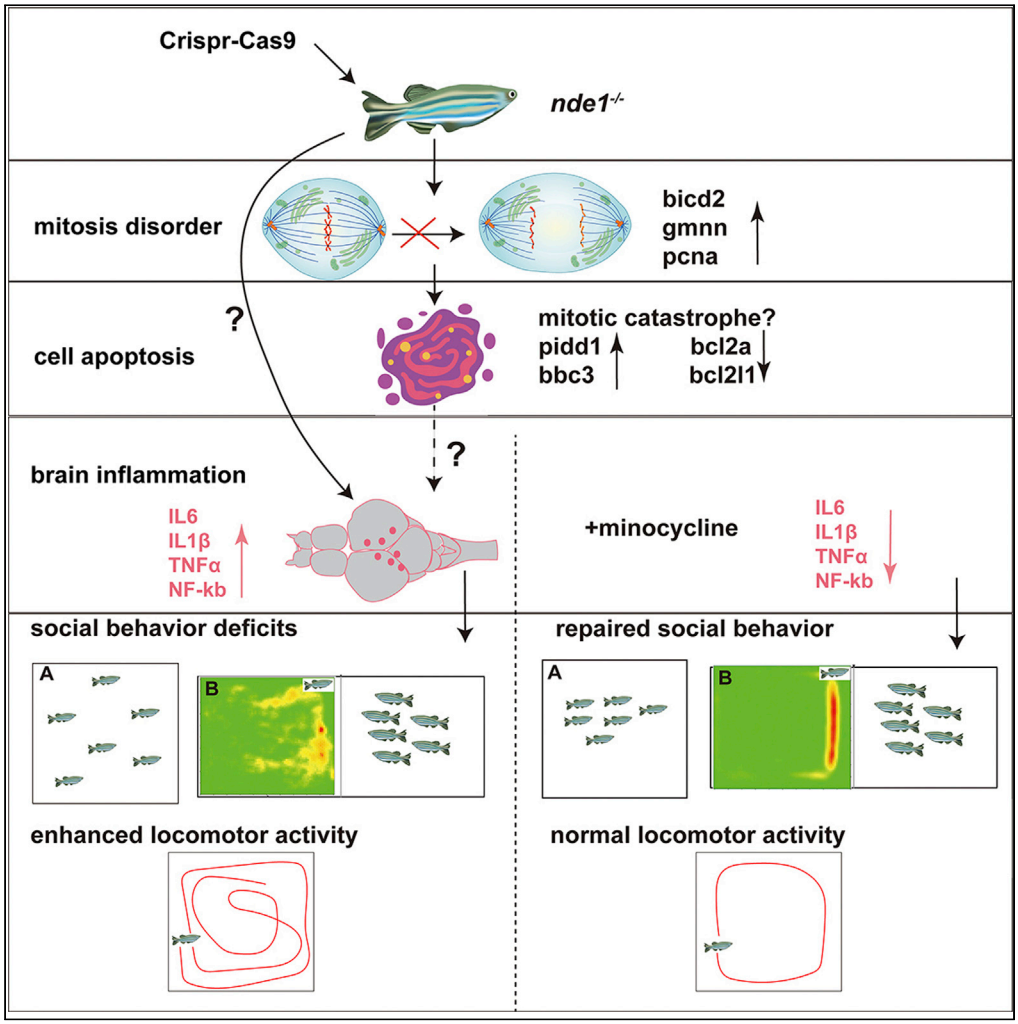

Qi Zhang, Tingting Li, Jia Lin, ..., Xudong Chen, Xu Wang, Qiang Li

liq@fudan.edu.cn

Highlights

nde1$^{-/-}$ zebrafish display autism-like behavior features

nde1 deficiency results in immune responses in the brain

Minocycline treatment inhibits immune responses in the adult *nde1*$^{-/-}$ brain

Minocycline rescued the impaired social behavior and locomotor activity

Zhang et al., iScience *25*, 103876
March 18, 2022
https://doi.org/10.1016/j.isci.2022.103876

iScience

CellPress
OPEN ACCESS

Article

Deficiency of *nde1* in zebrafish induces brain inflammatory responses and autism-like behavior

Qi Zhang,[1,5] Tingting Li,[1,5] Jia Lin,[1] Yinglan Zhang,[1] Fei Li,[1] Xudong Chen,[1] Xu Wang,[2,3,4] and Qiang Li[1,6,*]

SUMMARY

The cytoskeletal protein NDE1 plays an important role in chromosome segregation, neural precursor differentiation, and neuronal migration. Clinical studies have shown that NDE1 deficiency is associated with several neuropsychiatric disorders including autism. Here, we generated *nde1* homologous deficiency zebrafish (*nde1*$^{-/-}$) to elucidate the cellular molecular mechanisms behind it. *nde1*$^{-/-}$ exhibit increased neurological apoptotic responses at early infancy, enlarged ventricles, and shrank valvula cerebelli in adult brain tissue. Behavioral analysis revealed that *nde1*$^{-/-}$ displayed autism-like behavior traits such as increased locomotor activity and repetitive stereotype behaviors and impaired social and kin recognition behaviors. Furthermore, *nde1* mRNA injection rescued apoptosis in early development, and minocycline treatment rescued impaired social behavior and overactive motor activity by inhibiting inflammatory cytokines. In this study, we revealed that *nde1* homozygous deletion leads to abnormal neurological development with autism-related behavioral phenotypes and that inflammatory responses in the brain are an important molecular basis behind it.

INTRODUCTION

NDE1 (nudE Nuclear Distribution E homologue1) is located within 16p13.11, a hotspot chromosome segment associated with neuropsychiatric disorders (Ramalingam et al., 2011). Several clinical studies have shown that copy number deletion and duplication variants in the *NDE1* region are associated with neuropsychiatric disorders (Bakircioglu et al., 2011; Borlot et al., 2017; Kirov et al., 2009; Ramalingam et al., 2011; Ullmann et al., 2007; Williams et al., 2010). Among which, deletions of *NDE1* are strongly associated with intellectual disability (ID), autism, epilepsy, microcephaly, and so on. In 2010, Reinhard et al. detected deletion mutations of the *NDE1* region in three patients with ID (Ullmann et al., 2007). In 2011, Ramalingam et al. reported four patients containing deletion mutations in the *NDE1* region with clinical features including autism (2/4), epilepsy (3/4), and developmental delay (4/4) (Ramalingam et al., 2011). In the same year, Bakircioglu et al. identified severe microcephaly with ID in the off-springs of three families with *NDE1* deletions (Bakircioglu et al., 2011). In 2013 and 2017, three cases of microcephaly that resulted from *NDE1* deletions were reported (Paciorkowski et al., 2013; Tan et al., 2017).

NDE1 encodes a cytoskeletal protein located in the centrosome that can act as part of the LIS1-NDE1-cytoplasmic kinesin complex (Hennah et al., 2007). This complex is responsible for transporting vesicles and other entities from the axon tip to the neuronal cell body, involved in the proliferation and differentiation of neuronal precursors, neuronal migration, and neurite outgrowth (Hennah et al., 2007; Lanctot et al., 2013). Specifically, NDE1 involved in mitosis cell-cycle-linked oscillatory movement of the nucleus of radial glia progenitor (RGP) cells, and *Nde1* knockout in mice results in abnormal cortical development (Doobin et al., 2016; Houlihan and Feng 2014). Knockdown of *nde1* in zebrafish by MO technique leads to a delay in cell-cycle re-entry that correlates with ciliary length (Feng and Walsh 2004; Kim et al., 2011). However, the cellular-molecular mechanisms associated with neuropsychiatric disorders remain incompletely elucidated.

The cortical development and overall structure of the zebrafish brain is similar to that of mammals. For instance, neuronal epithelial cells of zebrafish proliferate to constitute the cortex through the interkinetic nuclear migration, similar to human (Leung et al., 2011). In addition, the immune system of zebrafish has almost all the lymphoid organs and immune cell types of mammals, the main innate immune signaling pathways such as TLR and NLR signaling pathways, and cytokines are conserved in zebrafish and mammals (Gomes and Mostowy 2020; Trede et al., 2004). A range of zebrafish motor behavior traits, such as

[1]Translational Medical Center for Development and Disease, Shanghai Key Laboratory of Birth Defect Prevention and Control, Institute of Pediatrics, Children's Hospital of Fudan University, National Children's Medical Center, Shanghai, 201102, China

[2]Cancer Institute, Pancreatic Cancer Institute, Fudan University Shanghai Cancer Center, Shanghai 200032, China

[3]Shanghai Pancreatic Cancer Institute, Shanghai Key Laboratory of Radiation Oncology, Fudan University Shanghai Cancer Center, Fudan University, Shanghai, 200032, China

[4]Key Laboratory of Metabolism and Molecular Medicine, Ministry of Education, School of Basic Medical Sciences, Fudan University, Shanghai, 200032, China

[5]These authors contributed equally

[6]Lead contact

*Correspondence: liq@fudan.edu.cn

https://doi.org/10.1016/j.isci.2022.103876

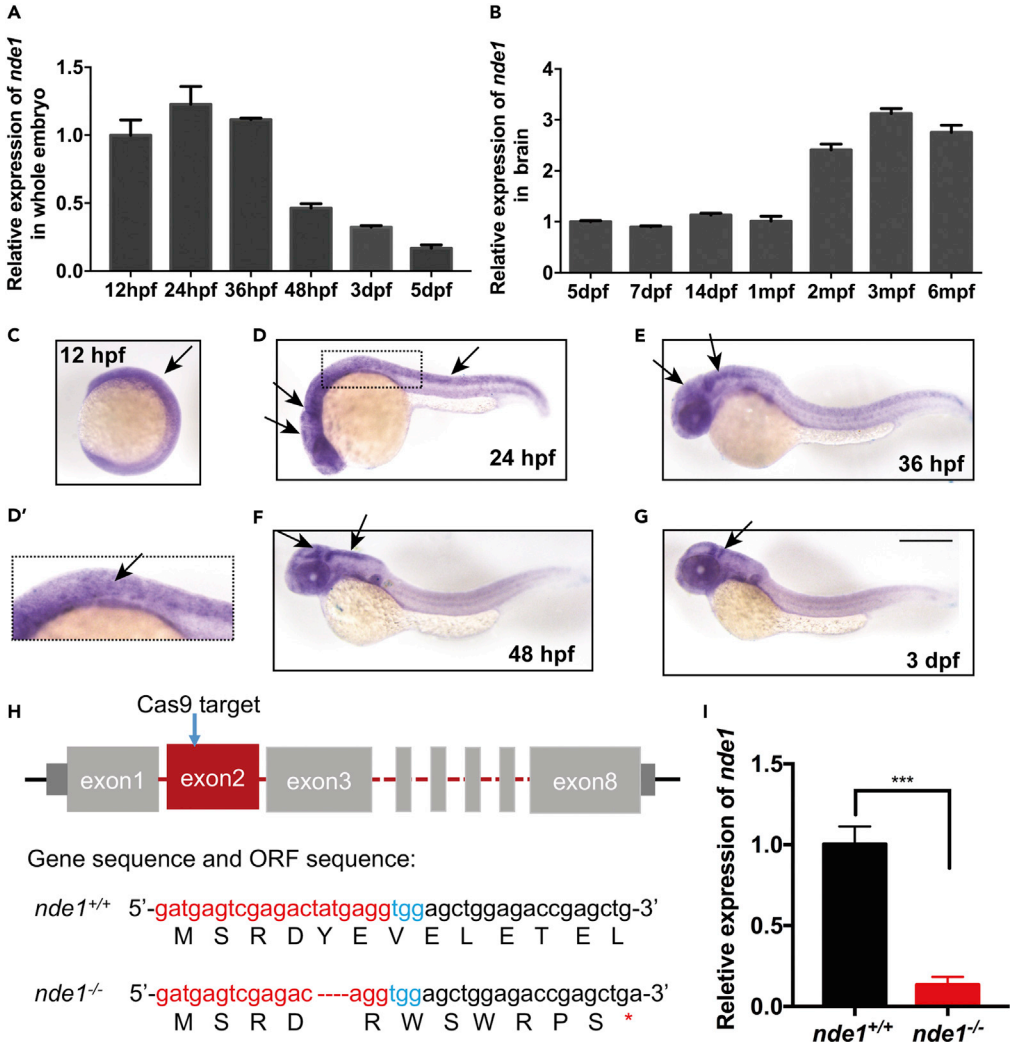

Figure 1. *nde1* Expression analysis and generation of *nde1* deficiency zebrafish

(A) Relative expression of *nde1* in zebrafish embryos during early development. Data are represented as mean ± SEM.

(B) Relative expression of *nde1* in zebrafish brain during five dpf to six mpf.

(C–G) Whole mount *in situ* hybridization of *nde1* during early development. Scale bar: 0.2 mm.

(D') Amplified images of boxed area in (D).

(H) Diagram of target site on second exon of zebrafish *nde1* genomic DNA, representative sequencing results and predicted ORF sequence of $nde1^{+/+}$ and $nde1^{-/-}$; red letter indicates N20 sequence; blue letter indicates NGG.

(I) Reduced expression of *nde1* mRNA in the brain of 6 mpf $nde1^{-/-}$ zebrafish. ***$p < 0.001$. Data are represented as mean ± SEM

spontaneous motor behavior, shoaling behavior, social behavior, repetitive stereotyped behavior, environmental adaptation, and aggressive behavior can serve as indicators of anxiety, depressive, pressure, or conflict symptoms (Geng and Peterson 2019; Kabashi et al., 2011). Hence, zebrafish are great models for pathogenesis research of neuropsychiatric disorders.

RESULTS

nde1 expression analysis in zebrafish during development

To investigate the expression pattern of *nde1* during development, we first analyzed the expression levels of *nde1* in zebrafish embryos or brain tissues at different time points. The results showed that *nde1* expression peaked at around 24 hpf-36 hpf (hours postfertilization) during early embryonic development and then decreased to one-fifth of 24 hpf expression levels at five dpf (days postfertilization) (Figure 1A). From five

dpf to one mpf (months postfertilization), the low level of *nde1* expression is maintained in the brain. At 2 mpf, when zebrafish enter young adulthood, *nde1* expression peaks second time and maintains such expression levels into adulthood (Figure 1B).

In situ hybridization analysis on early development embryos was consistent with expression quantification results. At 12 hpf, *nde1* was broadly expressed in the brain primordium and somites (Figure 1C). At 24 hpf, *nde1* was abundantly expressed in the nervous system, especially in the midbrain, hindbrain, and spinal cord (Figure 1D, arrows); magnified images in Figure 1D' displayed the widespread expression of *nde1* in the hindbrain and spinal cord. At 36 hpf and 48 hpf, *nde1* expression in the midbrain and hindbrain persisted. From 36 hpf, *nde1* expression in the spinal cord was diminished and eventually disappeared at 48 hpf. At three dpf, *nde1* was only minimally expressed in the mid-hindbrain boundary (Figures 1E–1G).

Generation of *nde1*-deficient zebrafish

We generated *nde1* knockout zebrafish using the CRISPR/Cas9 system. 20 nt *nde1* gene-specific guide RNA was designed to target the second exon. Genotyping of target PCR products after two generations of heterozygotes cross-confirmed that targeting allele carries a 4bp (TATG) deletion (Figures 1H and S1). The deletion resulted in a frameshift mutation and generates an early stop codon in exon 2 (Figure 1H). RT-qPCR analysis confirmed that *nde1* mRNA expression was significantly reduced in $nde1^{-/-}$ zebrafish (Figure 1I). These results indicate that we have successfully generated an *nde1*-deficient zebrafish transgenic line.

Morphological analysis and apoptosis analysis of $nde1^{-/-}$

To further investigate the effect of *nde1* knockout on zebrafish embryonic development, we performed morphological analysis and apoptosis analysis of $nde1^{-/-}$. During $nde1^{-/-}$ development, no significant cosmetic malformations were observed (data not shown), whereas at 30hpf, the $nde1^{-/-}$ nervous system, including telencephalon, midbrain, rhombomere, and spine, exhibited increased apoptosis (Figure 2A). Statistical analysis also showed a significant increase in apoptotic bodies in $nde1^{-/-}$ (Figure 2B).

Subsequently, we performed anatomical analysis for adult $nde1^{+/+}$ and $nde1^{-/-}$ zebrafish; the brain size and weight both showed no significant differences (Figure S2). Further analysis with HE-stained paraffin sections revealed the brains of adult $nde1^{-/-}$ exhibited relatively loosened structure, enlarged ventricles (Figure 2C, black arrow), and reduced valvula cerebelli (Figure 2C, red arrow). Figure S3 showed sections of three additional independent experiments. These results suggest that *nde1* knockout leads to increased apoptosis in early development and abnormal brain structure.

Locomotor activities of $nde1^{-/-}$ zebrafish at five dpf, two mpf, and three mpf

Neuropsychiatric disorders are mainly manifested by abnormal behavior phenotype. To determine whether the loss of function of *nde1* affects the locomotor activities during development, we performed the behavioral analysis at 5dpf (early childhood), 2mpf (young adulthood), and 3mpf (adulthood).

Figure 3A shows the experimental timing settings of analysis of 5dpf zebrafish locomotor activities. Firstly, locomotor activities of 25 min adaptation period (AP) and then 30 min activity stabilization period (ASP) were recorded. Then, we set up two light-dark switch cycles (5 min 100 lx for brightness and 5 min 0 lx for dark for one cycle) to detect the response of zebrafish under light variation. Results showed that the average swimming distances per minute of $nde1^{-/-}$ is significantly higher than that of $nde1^{+/+}$ throughout the whole experiment (Figures 3B and 3C). Under the two light-dark switch cycles, $nde1^{-/-}$ zebrafish displayed the same light-dark responses as the wild type (Figure 3B). We also analyzed the activity frequency of ASP at three intensity scales, 0–40 as low intensity, 40–80 as medium intensity, and 80–120 as high intensity. $nde1^{-/-}$ shows decreased low intensity activities and increased medium and high intensity activities (Figure 3D).

At two mpf and three mpf, locomotor activities were analyzed under light condition for 30 min, with AP for the first 10 min and ASP for the last 20 min. Results were consistent with that of five dpf; the average swimming distances per minute of $nde1^{-/-}$ were significantly higher than that of $nde1^{+/+}$ (Figures 3E–3G, comparison of 20 min ASP of locomotor activity of 3 mpf; see Figure S4).

When the swimming trajectories of zebrafish were analyzed by the software, we noticed that repetitive behaviors of two mpf and three mpf $nde1^{-/-}$ zebrafish, including back and forth, big circling, and small circling, exhibited a significantly higher frequency than $nde1^{+/+}$ (Figures 3H–3J).

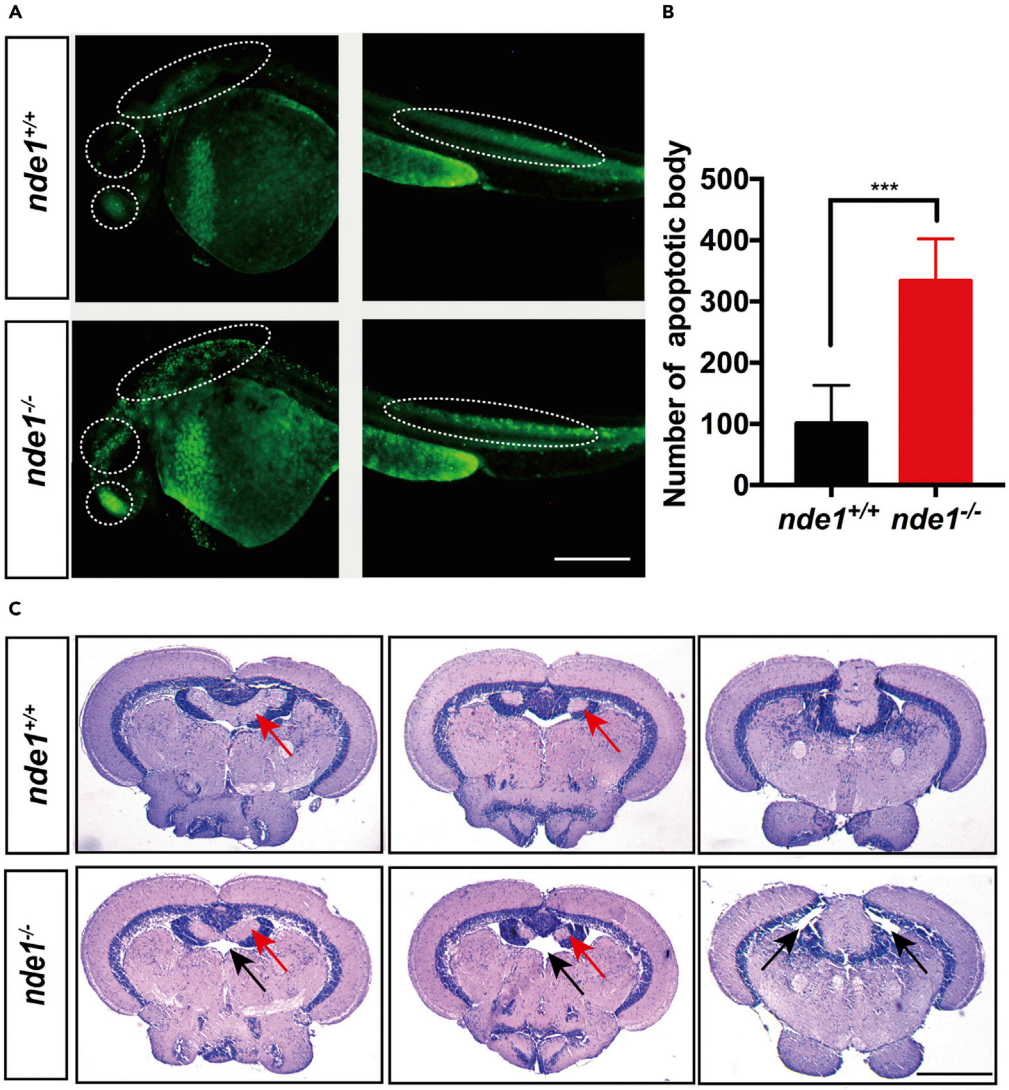

Figure 2. Morphological analysis and apoptosis analysis of *nde1*$^{-/-}$

(A) AO staining of *nde1*$^{+/+}$ and *nde1*$^{-/-}$ at 30hpf; white dotted oval indicates telencephalon, midbrain, rhombomere, and spine, respectively. Scale bar: 0.2 mm.

(B) Statistics of apoptotic bodies after AO staining in *nde1*$^{+/+}$ and *nde1*$^{-/-}$.

(C) HE-stained paraffin sections of midbrain of *nde1*$^{+/+}$ and *nde1*$^{-/-}$. Black arrow indicates the gaps between the ventricles; red arrow indicates valvula cerebelli. Scale bar: 0.5 mm. *p < 0.05, **p < 0.01, ***p < 0.001. Data are represented as mean ± SEM

Social behavior analysis of *nde1*$^{-/-}$ zebrafish at 2 mpf and 3 mpf

Zebrafish usually swim in clusters, and single fish tend to join groups of zebrafish of the same species (Spence et al., 2008). This characteristic of zebrafish can be used as a metric for its social activity. In order to explore the impact of *nde1* knockout on social behavior of *nde1*$^{-/-}$, we further analyzed the shoaling behavior, social preference, and kin preference. Each analysis lasts for 30 min, with AP for the first 10 min and ASP for the last 20 min.

In shoaling behavior analysis, the interindividual distance between populations of *nde1*$^{-/-}$ zebrafish at two mpf and three mpf was significantly higher than that of wild type, indicating that the population homogeneity of *nde1*$^{-/-}$ was impaired (Figures 4A–4B). In the analysis of social preference behavior, two mpf and three mpf *nde1*$^{-/-}$ zebrafish both spend significantly shorter time and distance in the social region (area 1)

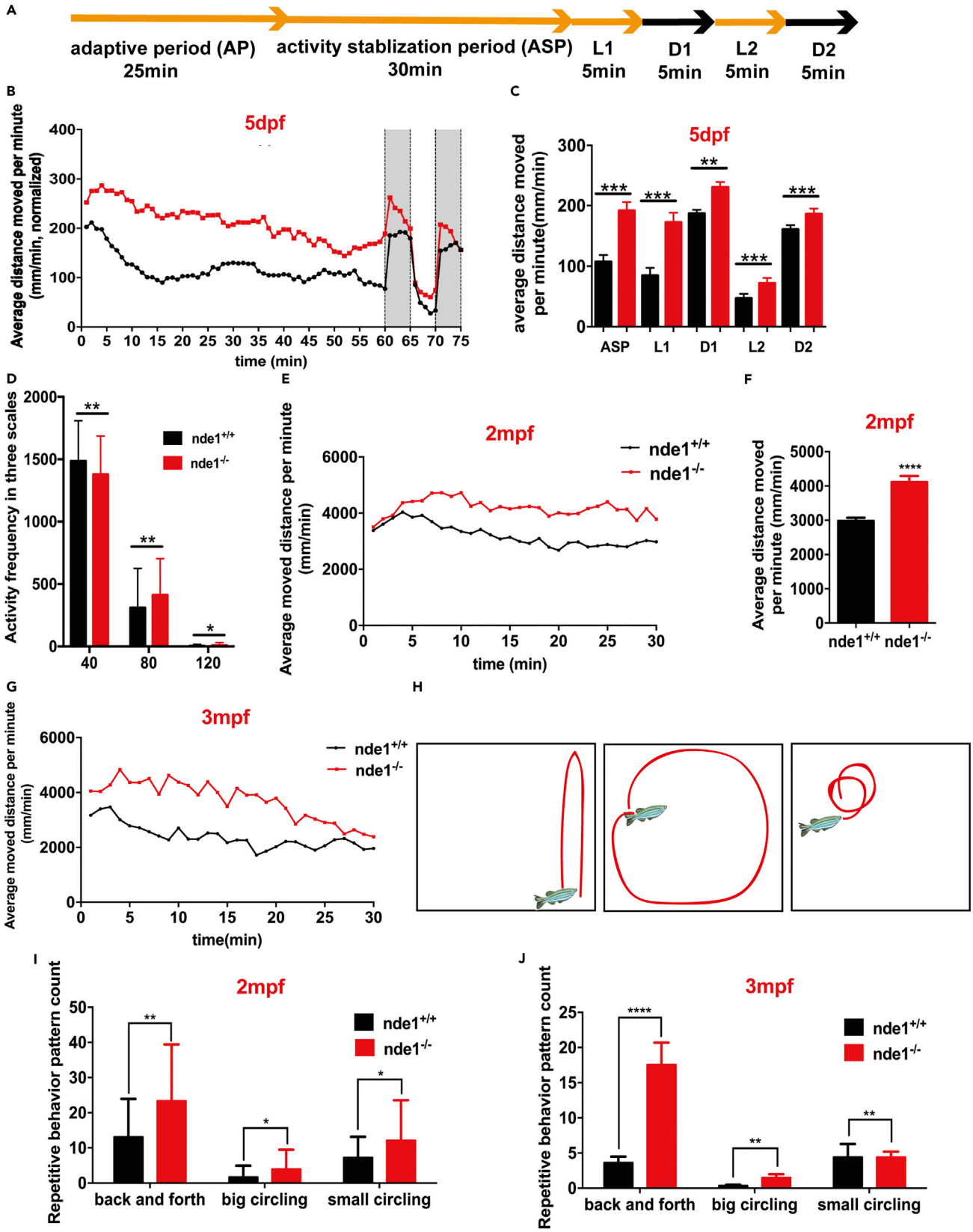
A
adaptive period (AP)
25min
activity stablization period (ASP)
30min
L1
5min
D1
5min
L2
5min
D2
5min
B
5dpf
Average distance moved per minute (mm/min, normalized)
time (min)
C
5dpf
average distance moved per minute(mm/min)
ASP
L1
D1
L2
D2
D
Activity frequency in three scales
nde1+/+
nde1-/-
E
2mpf
Average moved distance per minute (mm/min)
time (min)
F
2mpf
Average distance moved per minute (mm/min)
G
3mpf
Average moved distance per minute (mm/min)
time(min)
H
I
2mpf
Repetitive behavior pattern count
back and forth
big circling
small circling
J
3mpf
Repetitive behavior pattern count
back and forth
big circling
small circling

Figure 3. Zebrafish locomotor activity at 5 dpf, 2 mpf, and 3 mpf

(A) Experimental setup of analysis of 5 dpf locomotor activity.

(B) *nde1*$^{+/+}$ and *nde1*$^{-/-}$ larvae (5 dpf) movement trend line graph within 75 min of the experiment time (n = 36).

(C) Comparison of locomotor activity between nde1 *nde1*$^{+/+}$ and *nde1*$^{-/-}$ larvae (5 dpf).

(D) Activity frequency of ASP at three intensity scales.

(E and G) 2 mpf (E, n = 32) and 3 mpf (G, n = 28) *nde1*$^{+/+}$ and *nde1*$^{-/-}$ zebrafish movement trend graph within 30 min of the experiment time.

(F) Comparison of 20 min ASP of locomotor activity of two mpf *nde1*$^{+/+}$ and *nde1*$^{-/-}$ zebrafish.

(H) Representative trace of back and forth, big circling and small circling of *nde1*$^{-/-}$ zebrafish.

(I and J) 2 mpf (I) and three mpf (J) *nde1*$^{-/-}$ zebrafish showed more repetitive behaviors than *nde1*$^{+/+}$.

Data are shown as mean ± SEM; *p < 0.05, **p < 0.01, ***p < 0.001, ****p < 0.0001.

compared with *nde1*$^{+/+}$. It indicates that for *nde1* knockout zebrafish, the group tendency is relatively weak in both adolescence and adulthood (Figures 4C and 4D).

In the kin recognition and preference test, *nde1*$^{-/-}$ adult zebrafish (n = 28) spent more time at the kin region (area 1, kin group was conspecific and same color) and spent less time and distance at the non-kin region (area 2, non-kin group was red zebrafish) (Figures 4E and 4F). This suggests that *nde1*$^{-/-}$ are inclined to recognize similar groups and exhibit low sociality.

Transcriptome analysis of *nde1* knockout zebrafish

Morphological, anatomical, and behavioral analyses suggest that *nde1* deletion mutations result in morphological and functional abnormalities in the nervous system. To further explore the underneath molecular mechanism, we performed transcriptome profiling and analyzed global gene expression patterns of the 2mpf zebrafish brain. Sample clustering analysis showed good homogeneity within both the control groups (*nde1*$^{+/+}$) and experimental groups (*nde1*$^{-/-}$) (Figure S5A).

As was shown in volcano plot of the gene expression profiles, *nde1* deficiency resulted in approximately 850 DE-Gs (p-adjust < 0.05 and |log2FC| ≥ 1.0), of which 484 genes were upregulated and 366 genes were downregulated (Figure 5A) (Table S1, Detailed information of DE-Gs, related to Figure 5A). GO clustering analysis showed that DE-Gs were mainly enriched in biological process such as regulation of RNA metabolic and biosynthetic (Figure S5B). KEGG clustering analysis revealed that differential genes were mainly enriched in immune disease and inflammation-related pathways, such as antigen processing and presentation, Legionellosis, and inflammatory bowel disease (Figure 5B). The KEGG pathway enrichment string map (Figure S6) showed genes that differ significantly in the enrichment pathway.

Analysis of enriched KEGG pathways and key node genes revealed significant increase in the expression of the inflammatory signaling molecule NF-kb and *apoeb*, marker gene of the main immune cells of brain, microglia. Of note, microglia are a primary source of pro-inflammatory cytokines in the brain (Miller et al. 2009), which prompt us to analyze the expression levels of inflammatory cytokines in brain. Results showed that interleukin-6 (IL-6), tumor necrosis factor alpha (TNF-α), IL-1β was significantly promoted, whereas IL-4 and IL-12 were unaffected in *nde1*$^{-/-}$ brain (Figure 5C). These results suggest that *nde1* mainly affects the expression levels of immune and inflammation-related pathways, especially inflammatory cytokines.

Analysis of mitosis, apoptosis, and microglia-development-related gene expression levels in early embryonic development

nde1 is involved in the mitotic process of nerve cells, and former results in this study showed *nde1* deficiency results in excessive apoptosis in nervous system. To investigate the molecular mechanisms behind this, we first analyzed the expression levels of genes related to mitosis and apoptosis in early embryonic development. Results showed that at 24 hpf, DNA replicator *pcna*, geminin DNA replication inhibitor *gmnn*, and *bicd2*, which recruited the dynein to the nuclear envelope during early G2, were all upregulated in *nde1*$^{-/-}$ embryos (Figure 6A).

We then analyzed the expression of the pro-apoptotic genes *pidd1* and *bbc3* and genes that inhibit apoptosis, *bcl2a*, and *bcl2l* at 30 hpf. The results were consistent with the phenotype, *pidd1* and *bbc3* were promoted, and *bcl2a* and *bcl2l* were inhibited in *nde1*$^{-/-}$ embryos (Figure 6B). After 60 hpf, macrophages in the brain began transforming into microglia and abruptly started expressing *apoeb* (Herbomel et al. 2001). Quantitative analysis results showed *nde1*$^{-/-}$ embryos express significantly higher expression level of *apoeb* at four dpf (Figure 6C).

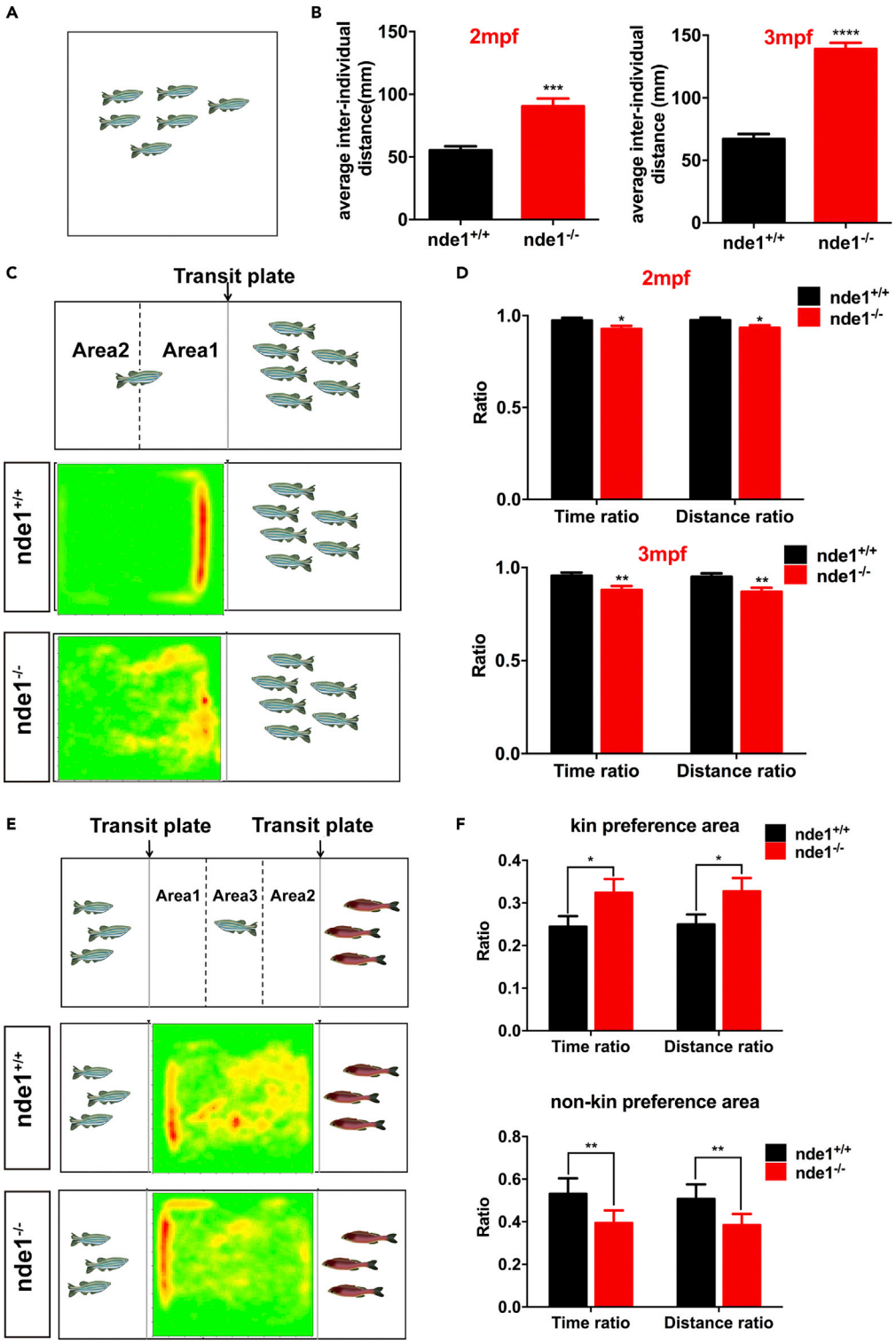

Figure 4. Social behavior analysis of *nde1*$^{-/-}$ zebrafish

(A) Schematic of shoaling test.

(B) Significantly increased inter-fish distance of 2 mpf (n = 10) and 3 mpf (n = 10) *nde1*$^{-/-}$ zebrafish.

(C) Schematic and representative heatmap of social preference test; area1: social area, area2: nonsocial area.

Figure 4. *Continued*

(D) Time ratio and distance ratio in the social area were significantly reduced in 2 mpf (n = 35) and 3 mpf (n = 28) *nde1*$^{-/-}$ zebrafish compared with *nde1*$^{+/+}$ zebrafish.

(E) Schematic and representative heatmap of kin recognition and preference test; area1: kin preference area, area2: nonkin preference area.

(F) Significantly increased ratio of kin preference area entering and decreased ratio of nonkin preference area entering in 3 mpf *nde1*$^{-/-}$ zebrafish (n = 28).

Data are presented as mean ± SEM; *p < 0.05, **p < 0.01, ***p < 0.001, ****p < 0.0001

Rescue of mitotic disorders and excessive apoptosis by *nde1* mRNA injection

Furthermore, we performed rescue experiments of *nde1* mRNA restoration in *nde1* knockout embryos. The results showed that at 24 hpf, upregulated *bicd2*, *gmnn*, and *pcna* were inhibited in mutant embryos with *nde1* mRNA supplementation, and *gmnn* and *pcna* were restored to normal expression levels (Figure 6A), whereas at 30 hpf, *pidd1* and *bbc3*, *bcl2a*, and *bcl2l* expression levels were also back to normal (Figure 6B); apoptotic bodies in the nervous system of *nde1*-rescue embryos were significantly reduced than *nde1*$^{-/-}$ (Figures 6D and 6E). At four dpf, the expression level of *apoeb* was significantly decreased compared with the *nde1*$^{-/-}$ but still significantly higher than the wild type (Figure 6C).

Rescue of behavior deficits and brain inflammation of *nde1*$^{-/-}$ zebrafish by minocycline

Minocycline (MC) is a tetracycline-derived antibiotic that could penetrate the blood-brain barrier and inhibits microglia activation. Previous research demonstrate that MC attenuates inflammation associated with microglial activation, decreases cytokines expression such as IL-1β, and inhibits nuclear factor NF-kb activation (Henry et al., 2008; Si et al., 2004).

In order to determine whether MC could inhibit the brain inflammatory response and rescue autism-like behavior in *nde1*-deficient zebrafish, we performed series of analysis. After MC immersion treatment for two weeks, expression of NF-kb, IL-6, TNF-α, and IL-1β in 3.5 mpf *nde1*$^{-/-}$ zebrafish brains were restored to normal levels (Figure 7A).

Then we analyzed the behavior performance of four experimental groups of zebrafish. The locomotor activities of *nde1*$^{-/-}$ were significantly higher than that of *nde1*$^{+/+}$, which was consistent with former result. After MC treatment, average swimming distances per minute of *nde1*$^{-/-}$ zebrafish showed no significant difference compared with control group *nde1*$^{+/+}$ (Figures 7B and 7C).

In shoaling behavior analysis, MC treated *nde1*$^{-/-}$ zebrafish showed rescued population homogeneity, the inter-individual distance between populations displayed no significantly difference from the control (Figure 7D). Repaired group tendency confirmed also by the analysis of social preference behavior, the total time and distances of MC-treated *nde1*$^{-/-}$ zebrafish swam in the social area did not differ from wild type (Figure 7E). These results indicate that MC treatment downregulated the overexpression of inflammatory cytokines in *nde1*$^{-/-}$ zebrafish and rescued their impaired social behavior and locomotor activity.

DISCUSSION

Increased locomotor activity is one of the behaviors that characterize anxiety in human (Maphanga et al., 2020). *nde1* deficiency results in increasement in locomotor activity that does not habituate over time. In tests of shoaling, social preference, and kin preference during youth and adulthood, *nde1*$^{-/-}$ zebrafish showed significantly reduced preference for groups and exhibited abnormal social novelty (Figure 4). In the open field, *nde1*$^{-/-}$ showed significantly increased repetitive behaviors such as back and forth (large circles and small circles) (Figure 3). Social deficits, repetitive behaviors, and hyperactivity are among the main clinical features of autism (Lai et al. 2014). These behaviors in *nde1* knockout zebrafish can be interpreted as autism-like behaviors. In addition, brain MRI imaging of autistic patients showed reduced cerebellum (Akshoomoff et al., 2004; Stigler et al., 2011), CT scans of patients with *NDE1* double allele variants showed variable degrees of shrank cerebral hemispheres and ventriculomegaly (Abdel-Hamid et al., 2019). The phenotypes of enlarged ventricles and reduced cerebellar valves of *nde1*$^{-/-}$ zebrafish were consistent with autism patients (Figure 2). This suggests that *nde1* knockout zebrafish can be used as a model for etiological studies of neuropsychiatric disorders such as autism caused by nde1 variants.

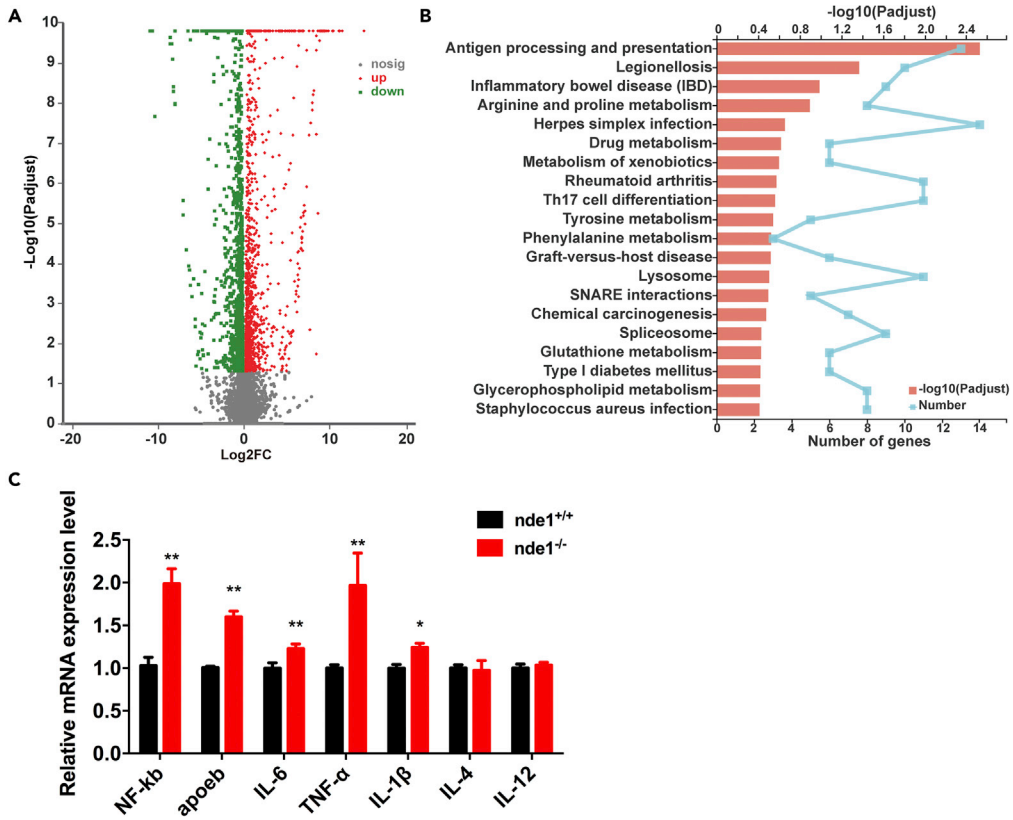

Figure 5. Transcriptome analysis of two mpf *nde1*$^{-/-}$ zebrafish brain tissue

(A) Volcano plot of the gene expression profiles. Gray plot indicates no significance; red plot indicates upregulated genes; green plot indicates downregulated genes.

(B) Twenty signaling pathways with the strongest significant differences in KEGG analysis.

(C) Inflammatory cytokine and immune molecules expression in two mpf zebrafish brain tissue (n = 5). Data are presented as mean ± SEM; *p < 0.05, **p < 0.01

NDE1/LIS1/dynein complex essentially organizes the mitotic spindle to control nuclear migration, cell-cycle progression, and mitosis (Bakircioglu et al., 2011; Soto-Perez et al. 2020). The depletion of NDE1 results in the failure of microtubules to focus on kinetochores, followed by impaired chromosome segregation (Vergnolle and Taylor 2007). In this study, *nde1* knockout zebrafish exhibit abnormal high expression of mitosis-related genes such as *bicd2*, *gmnn*, and *pcna* during early embryonic development (Figure 6A), as well as increased expression of genes that promote apoptosis such as *pidd1*, *bbc3* and decreased expression of genes that inhibit apoptosis such as *bcl2a*, *bcl2l* (Figure 6B). In mice, *Nde1* mutants have been found to cause DNA damage, leading to the activation of *p53*-dependent apoptosis and affecting the differentiation of neural progenitor cells (Pei et al., 2014). In the brains of autistic patients, increased apoptosis was detected in both the frontal cortex and cerebellum with downregulation of *Bcl2* (Araghi-Niknam and Fatemi, 2003; Malik et al., 2011; Sheikh et al., 2010). We hypothesize that *nde1* mutations may trigger mitotic catastrophe, a mechanism that senses mitotic failure and subsequently drives cells into apoptotic or necrotic steps (Vitale et al., 2011). This speculation was partially supported by the *nde1* mRNA rescue assay, in which the number of apoptotic cells in the nervous system was dramatically reduced after mitosis-related gene expression was restored to normal levels (Figure 6).

There is growing evidence that the immune system plays an important role in brain development and individual life behaviors. Inflammatory cytokines affect brain development, and most neurodevelopmental disorders such as autism, cognitive impairment, cerebral palsy, epilepsy, and schizophrenia are associated with early inflammation (Jiang et al., 2018). Some autistic patients exhibited enhanced neuroinflammatory responses with elevated expression of IL-6, HSP70, TGF-β2, Caspase 7, and INF-γ (El-Ansary and Al-Ayadhi 2012; Wei et al., 2011). In our study, *nde1*$^{-/-}$ zebrafish expressed high levels of

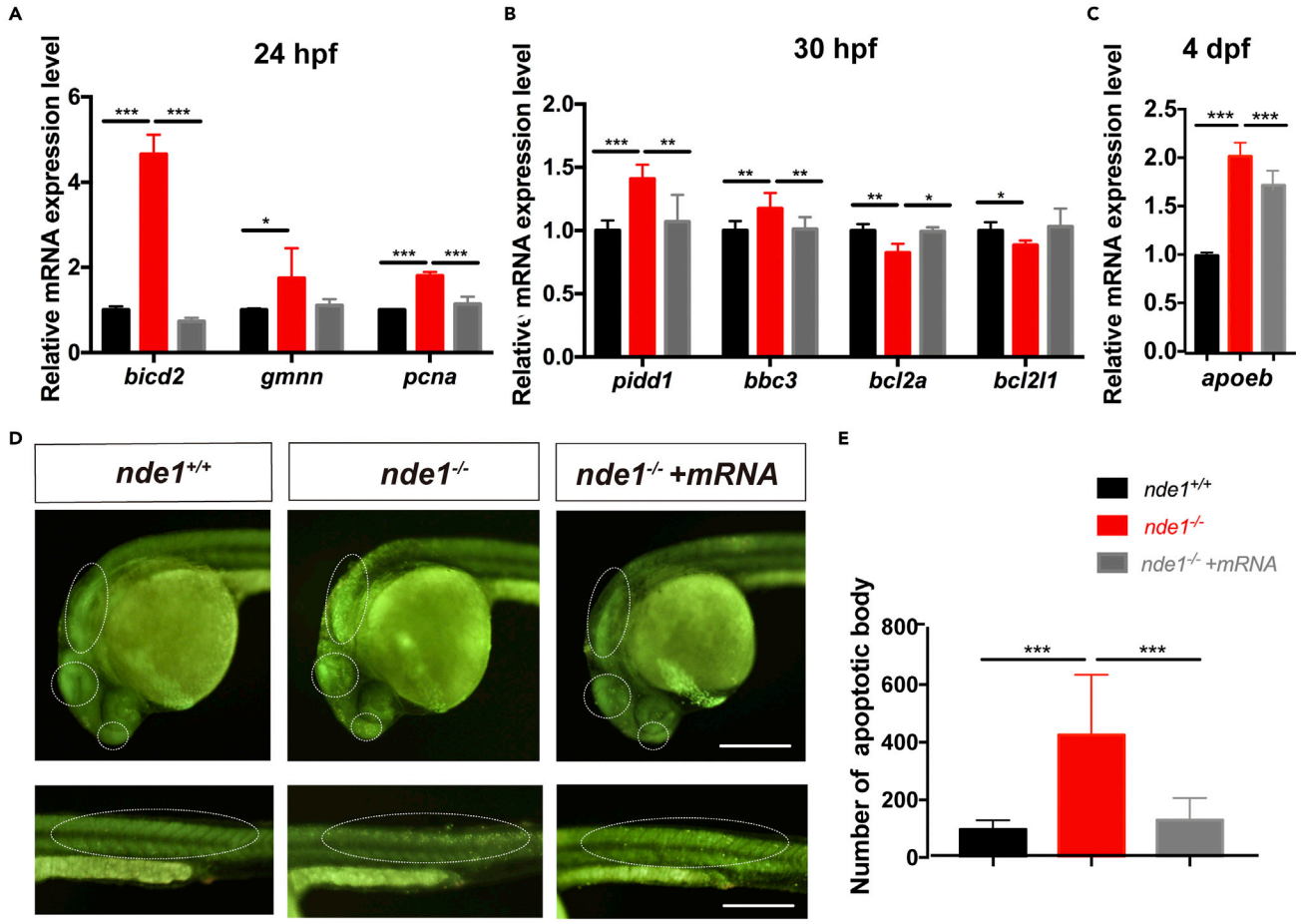

Figure 6. *nde1* mRNA rescue mitosis, apoptosis, and immune-related phenotype

(A–C). Relative expression level of *bicd2, gmnn*, *pcna*, *pidd1*, *bbc3*, *bcl2a*, and *bcl2l1*, *apoeb* in $nde1^{+/+}$, $nde1^{-/-}$, and nde1 mRNA rescued zebrafish.

(D) AO staining of $nde1^{+/+}$, $nde1^{-/-}$, and *nde1* mRNA rescued zebrafish at 28 hpf. White dotted oval indicates telencephalon, midbrain, rhombomere, and spine, respectively. Scale bar: 0.2 mm.

(E) Statistics of apoptotic bodies after AO staining.

*p < 0.05, **p < 0.01, ***p < 0.001. Data are presented as mean ± SEM

microglia marker gene *apoeb* in both early developmental and adult brains (Figures 5C and 6C). Transcriptomic analysis of adult $nde1^{-/-}$ brains showed the affected pathway was enriched in immune processes, with high levels of expression of pro-inflammatory cytokine IL-6, TNF-α, IL-1β, and immune signaling molecule NF-kb (Figures 5B and 5C). Introduction of *nde1* mRNA only partially rescued the up-regulated *apoeb* at 4 dpf, which could be that *nde1* mRNA was depleted during development, resulting in incomplete restoration of *apoeb* to normal levels. Previous studies showed that IL-1β and TNF-α induce neuronal cell death *in vivo* (Fricker et al., 2018; Matelski et al., 2021). Here in our study, apoptosis occurs earlier in development than the inflammatory response; the inflammatory response could be induced by apoptosis or other reasons.

Taking advantage of the characteristics of minocycline crossing the blood-brain barrier to inhibit microglia activation and inflammatory cytokines, we initially explored the association between brain inflammatory response and autistic-like behavior. The results revealed that the expression of inflammatory factors IL-6, TNF-α, IL-1β, and NF-kb was restored to normal (Figure 7A). More importantly, impaired social behaviors and locomotor activity were also restored to wild-type levels (Figure 7B). Recent studies generated several inferences about how cytokines and microglia are involved in the mechanisms of CNS development and function. Cytokines in the CNS may negatively regulate activity-dependent synaptic pruning by interacting with MHCI; microglia are also involved in functional neuronal pruning and in the regulation of synaptic

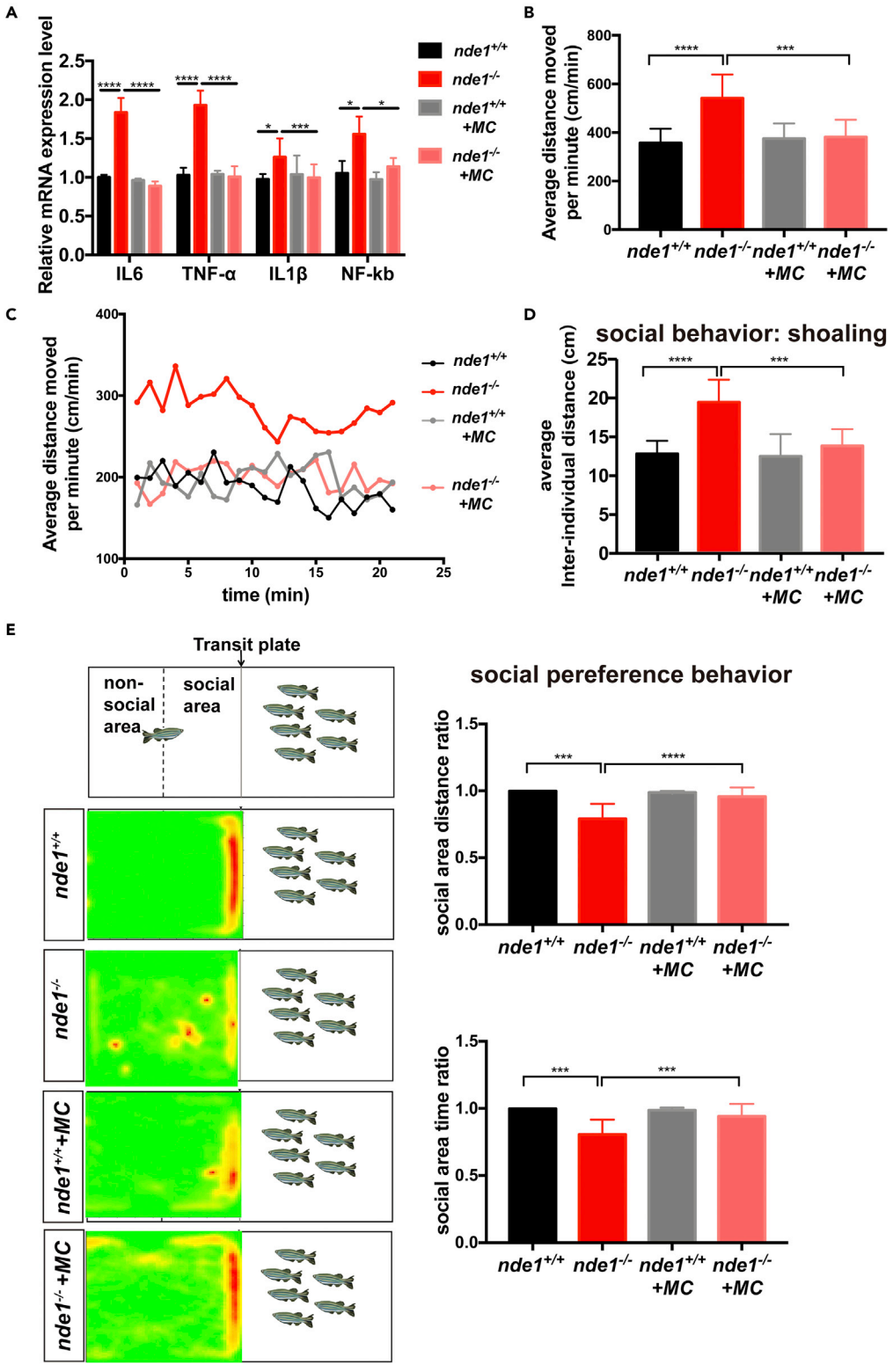
A
Relative mRNA expression level
2.5
2.0
1.5
1.0
0.5
0.0
IL6
TNF-α
IL1β
NF-kb
nde1+/+
nde1-/-
nde1+/+ +MC
nde1-/- +MC
B
Average distance moved per minute (cm/min)
800
600
400
200
0
nde1+/+
nde1-/-
nde1+/+ +MC
nde1-/- +MC
C
Average distance moved per minute (cm/min)
400
300
200
100
0
5
10
15
20
25
time (min)
D
social behavior: shoaling
average Inter-individual distance (cm)
25
20
15
10
5
0
E
Transit plate
non-social area
social area
nde1+/+
nde1-/-
nde1+/+ +MC
nde1-/- +MC
social pereference behavior
social area distance ratio
1.5
1.0
0.5
0.0
social area time ratio

Figure 7. Analysis of brain inflammatory response and behavior of minocycline treated zebrafish

(A) Relative expression level of IL-6, TNF-α, IL-1β, and NF-kb in *nde1*$^{+/+}$, *nde1*$^{-/-}$, and minocycline-treated zebrafish.

(B and C) Locomotor activity (B) and movement trend graph (C) of 3.5 mpf *nde1*$^{+/+}$, *nde1*$^{-/-}$, *nde1*$^{+/+}$ treated with MC, and *nde1*$^{-/-}$ treated with MC, n = 12.

(D) Inter-fish distance of four groups of zebrafish in shoaling behavior analysis (n = 10).

(E) Schematic and representative heatmap of social preference test.

Time ratio and distance ratio in the social area were displayed (n = 10). *p < 0.05, **p < 0.01, ***p < 0.001, ****p < 0.0001. Data are presented as mean ± SEM

plasticity in cognitive processes such as learning and memory (Miller et al. 2009). Another theory states that cytokines may influence human behavior by activating the hypothalamic-pituitary-adrenal axis and stimulating the secretion of pro-adrenocorticotropic hormones, arginine vasopressin, and corticosterone. In the context of overactive microglia responses, excessive amounts of pro-inflammatory cytokines have been shown to induce excitotoxicity and neuronal death (Jiang et al., 2018).

Limitations of the study

Our work demonstrates *nde1* deletion mutation results in autistic behavioral phenotype similar to that of human in zebrafish, and increased immune response and apoptosis in brain are molecular basis behind the autism-like behavior. The MC rescue experiment indicates immune response inhibition across the blood-brain barrier could act as a candidate therapeutic pathway in *nde1*-deficiency-resulted autism. However, the pathogenic mechanisms behind inflammatory responses lead to behavioral abnormalities, and how the *nde1* mutation leads to inflammatory responses in the brain need further research.

ETHICS APPROVAL AND CONSENT TO PARTICIPATE

All procedures are approved by the institutional animal care committee of Children's Hospital of Fudan University, China.

STAR★METHODS

Detailed methods are provided in the online version of this paper and include the following:

- KEY RESOURCES TABLE
- RESOURCE AVAILABILITY
  - Lead contact
  - Material availability
  - Data and code availability
- EXPERIMENT MODEL AND SUBJECT DETAILS
  - Animals
- METHOD DETAILS
  - Synthesis of Digoxigenin-labeled RNA probe and whole mount *in* situ hybridization
  - Generation of *nde1*$^{-/-}$ zebrafish using CRISPR/Cas9
  - Acridine orange (AO) staining
  - Brain weighing
  - Paraffin sections
  - Hematoxylin-eosin (HE) staining
  - Transcriptome resequencing analysis (RNA-seq)
  - RNA isolation, real-time PCR (qPCR)
  - Capped *nde1* mRNA synthesis
  - Microinjection
  - Behavioral experiments
  - Larval activity
  - Open-field locomotor activity test
  - Shoaling test
  - Social preference test
  - Kin preference test
  - Minocycline treatment
- QUANTIFICATION AND STATISTICAL ANALYSIS

SUPPLEMENTAL INFORMATION

Supplemental information can be found online at https://doi.org/10.1016/j.isci.2022.103876.

ACKNOWLEDGMENTS

This work was supported by grants from the National Natural Science Foundation of China (NSFC, no. 81771632 and no. 81271509) to Qiang Li and Natural Science Foundation of Shanghai (21ZR1410100) to Qiang Li. We thank Children's Hospital of Fudan University for the support.

AUTHORS CONTRIBUTIONS

Conceptualization: QZ, TTL, QL. Methodology: QZ, TTL, JL, YLZ. Investigation: QZ, JL, YLZ, FL. Visualization: QZ, JL, XDC. Supervision: XW, QL. Writing—Original Draft: QZ, TTL, QL. Writing—Review & Editing: QZ, QL

DECLARATION OF INTERESTS

Authors declare that they have no competing interests.

Received: July 27, 2021
Revised: January 10, 2022
Accepted: February 1, 2022
Published: March 18, 2022

REFERENCES

Abdel-Hamid, M.S., El-Dessouky, S.H., Ateya, M.I., Gaafar, H.M., and Abdel-Salam, G.M.H. (2019). Phenotypic spectrum of NDE1-related disorders: from microlissencephaly to microhydranencephaly. Am. J. Med. Genet. A *179*, 494–497.

Akshoomoff, N., Lord, C., Lincoln, A.J., Courchesne, R.Y., Carper, R.A., Townsend, J., and Courchesne, E. (2004). Outcome classification of preschool children with autism spectrum disorders using MRI brain measures. J. Am. Acad. Child Adolesc. Psychiatry *43*, 349–357.

Araghi-Niknam, M., and Fatemi, S.H. (2003). Levels of bcl-2 and P53 are altered in superior frontal and cerebellar cortices of autistic subjects. Cell Mol. Neurobiol. *23*, 945–952.

Bakircioglu, M., Carvalho, O.P., Khurshid, M., Cox, J.J., Tuysuz, B., Barak, T., Yilmaz, S., Caglayan, O., Dincer, A., Nicholas, A.K., Quarrell, O., Springell, K., Karbani, G., Malik, S., Gannon, C., Sheridan, E., Crosier, M., Lisgo, S.N., Lindsay, S., Bilguvar, K., Gergely, F., Gunel, M., and Woods, C.G. (2011). The essential role of centrosomal NDE1 in human cerebral cortex neurogenesis. Am. J. Hum. Genet. *88*, 523–535.

Borlot, F., Regan, B.M., Bassett, A.S., Stavropoulos, D.J., and Andrade, D.M. (2017). Prevalence of pathogenic copy number variation in adults with pediatric-onset epilepsy and intellectual disability. JAMA Neurol. *74*, 1301–1311.

Doobin, D.J., Kemal, S., Dantas, T.J., and Vallee, R.B. (2016). Severe NDE1-mediated microcephaly results from neural progenitor cell cycle arrests at multiple specific stages. Nat. Commun. *7*, 12551.

El-Ansary, A., and Al-Ayadhi, L. (2012). Neuroinflammation in autism spectrum disorders. J. Neuroinflammation *9*, 265.

Feng, Y., and Walsh, C.A. (2004). Mitotic spindle regulation by Nde1 controls cerebral cortical size. Neuron *44*, 279–293.

Fricker, M., Tolkovsky, A.M., Borutaite, V., Coleman, M., and Brown, G.C. (2018). Neuronal cell death. Physiol. Rev. *98*, 813–880.

Geng, Y., and Peterson, R.T. (2019). The zebrafish subcortical social brain as a model for studying social behavior disorders. Dis. Model Mech. *12*, dmm039446.

Gomes, M.C., and Mostowy, S. (2020). The case for modeling human infection in zebrafish. Trends Microbiol. *28*, 10–18.

Hennah, W., Tomppo, L., Hiekkalinna, T., Palo, O.M., Kilpinen, H., Ekelund, J., Tuulio-Henriksson, A., Silander, K., Partonen, T., Paunio, T., Terwilliger, J.D., Lönnqvist, J., and Peltonen, L. (2007). Families with the risk allele of DISC1 reveal a link between schizophrenia and another component of the same molecular pathway, NDE1. Hum. Mol. Genet. *16*, 453–462.

Henry, C.J., Huang, Y., Wynne, A., Hanke, M., Himler, J., Bailey, M.T., Sheridan, J.F., and Godbout, J.P. (2008). Minocycline attenuates lipopolysaccharide (LPS)-Induced neuroinflammation, sickness behavior, and anhedonia. J. Neuroinflammation *5*, 15.

Herbomel, P., Thisse, B., and Thisse, C. (2001). Zebrafish early macrophages colonize cephalic mesenchyme and developing brain, retina, and epidermis through a M-CSF receptor-dependent invasive process. Dev. Biol. *238*, 274–288.

Houlihan, S.L., and Feng, Y. (2014). The scaffold protein Nde1 safeguards the brain genome during S phase of early neural progenitor differentiation. Elife *3*, e03297.

Ji, Y., Lin, J., Peng, X., Liu, X., Li, F., Zhang, Y., Guo, N., and Li, Q. (2017). Behavioural responses of zebrafish larvae to acute ethosuximide exposure. Behav. Pharmacol. *28*, 428–440.

Jiang, N.M., Cowan, M., Moonah, S.N., and Petri, W.A., Jr. (2018). The impact of systemic inflammation on neurodevelopment. Trends Mol. Med. *24*, 794–804.

Kabashi, E., Brustein, E., Champagne, N., and Drapeau, P. (2011). Zebrafish models for the functional genomics of neurogenetic disorders. Biochim. Biophys. Acta *1812*, 335–345.

Kim, S., Zaghloul, N.A., Bubenshchikova, E., Oh, E.C., Rankin, S., Katsanis, N., Obara, T., and Tsiokas, L. (2011). Nde1-Mediated inhibition of ciliogenesis affects cell cycle Re-entry. Nat. Cell Biol. *13*, 351–360.

Kirov, G., Grozeva, D., Norton, N., Ivanov, D., Mantripragada, K.K., Holmans, P., Craddock, N., Owen, M.J., and O'Donovan, M.C. (2009). Support for the involvement of large copy number variants in the pathogenesis of schizophrenia. Hum. Mol. Genet. *18*, 1497–1503.

Lai, M.-C., Lombardo, M.V., and Baron-Cohen, S. (2014). Autism. Lancet (London, England) *383*, 896–910.

Lanctot, A.A., Peng, C.Y., Pawlisz, A.S., Joksimovic, M., and Feng, Y. (2013). Spatially dependent dynamic MAPK modulation by the nde1-lis1-Brap complex patterns mammalian CNS. Dev. Cell *25*, 241–255.

Leung, L., Klopper, A.V., Grill, S.W., Harris, W.A., and Norden, C. (2011). Apical migration of nuclei during G2 is a prerequisite for all nuclear motion in zebrafish neuroepithelia. Development *138*, 5003–5013.

Li, Q., Lin, J., Zhang, Y., Liu, X., Chen, X.Q., Xu, M.Q., He, L., Li, S., and Guo, N. (2015). Differential behavioral responses of zebrafish larvae to

Yohimbine treatment. Psychopharmacology (Berl) *232*, 197–208.

Liu, C.X., Li, C.Y., Hu, C.C., Wang, Y., Lin, J., Jiang, Y.H., Li, Q., and Xu, X. (2018). CRISPR/Cas9-Induced Shank3b mutant zebrafish display autism-like behaviors. Mol. Autism *9*, 23.

Malik, M., Sheikh, A.M., Wen, G., Spivack, W., Brown, W.T., and Li, X. (2011). Expression of inflammatory cytokines, Bcl2 and cathepsin D are altered in lymphoblasts of autistic subjects. Immunobiology *216*, 80–85.

Maphanga, V.B., Skalicka-Woźniak, K., Budzynska, B., Enslin, G.M., and Viljoen, A.M. (2020). Screening selected medicinal plants for potential anxiolytic activity using an in vivo zebrafish model. Psychopharmacology (Berl) *237*, 3641–3652.

Matelski, L., Morgan, R.K., Grodzki, A.C., Van de Water, J., and Lein, P.J. (2021). Effects of cytokines on nuclear factor-Kappa B, cell viability, and synaptic connectivity in a human neuronal cell line. Mol. Psychiatry *26*, 875–887.

Miller, A.H., Maletic, V., and Raison, C.L. (2009). Inflammation and its discontents: the role of cytokines in the pathophysiology of major depression. Biol. Psychiatry *65*, 732–741.

Paciorkowski, A.R., Keppler-Noreuil, K., Robinson, L., Sullivan, C., Sajan, S., Christian, S.L., Bukshpun, P., Gabriel, S.B., Gleeson, J.G., Sherr, E.H., and Dobyns, W.B. (2013). Deletion 16p13.11 uncovers NDE1 mutations on the non-deleted homolog and extends the spectrum of severe microcephaly to include fetal brain disruption. Am J Med Genet A *161A* (7), 1523–1530.

Pei, Z., Lang, B., Fragoso, Y.D., Shearer, K.D., Zhao, L., Mccaffery, P.J., Shen, S., Ding, Y.Q., McCaig, C.D., and Collinson, J.M. (2014). The expression and roles of Nde1 and Ndel1 in the adult mammalian central nervous system. Neuroscience *271*, 119–136.

Ramalingam, A., Zhou, X.G., Fiedler, S.D., Brawner, S.J., Joyce, J.M., Liu, H.Y., and Yu, S. (2011). 16p13.11 duplication is a risk factor for a wide spectrum of neuropsychiatric disorders. J. Hum. Genet. *56*, 541–544.

Sheikh, A.M., Li, X., Wen, G., Tauqeer, Z., Brown, W.T., and Malik, M. (2010). Cathepsin D and apoptosis related proteins are elevated in the brain of autistic subjects. Neuroscience *165*, 363–370.

Si, Q., Cosenza, M., Kim, M.O., Zhao, M.L., Brownlee, M., Goldstein, H., and Lee, S. (2004). A novel action of minocycline: inhibition of human immunodeficiency virus type 1 infection in microglia. J. Neurovirol. *10*, 284–292.

Soto-Perez, J., Baumgartner, M., and Kanadia, R.N. (2020). Role of NDE1 in the development and evolution of the Gyrified cortex. Front. Neurosci. *14*, 617513.

Spence, R., Gerlach, G., Lawrence, C., and Smith, C. (2008). The behaviour and ecology of the zebrafish, Danio rerio. Biol. Rev. Camb. Philos. Soc. *83*, 13–34.

Stigler, K.A., McDonald, B.C., Anand, A., Saykin, A.J., and McDougle, C.J. (2011). Structural and functional magnetic resonance imaging of autism spectrum disorders. Brain Res. *1380*, 146–161.

Tan, L., Bi, B., Zhao, P., Cai, X., Wan, C., Shao, J., and He, X. (2017). Severe congenital microcephaly with 16p13.11 microdeletion combined with NDE1 mutation, a case report and literature review. BMC Med. Genet. *18*, 141.

Thisse, C., and Thisse, B. (2008). High-resolution in situ hybridization to whole-mount zebrafish embryos. Nat. Protoc. *3*, 59–69.

Trede, N.S., Langenau, D.M., Traver, D., Look, A.T., and Zon, L.I. (2004). The use of zebrafish to understand immunity. Immunity *20*, 367–379.

Ullmann, R., Turner, G., Kirchhoff, M., Chen, W., Tonge, B., Rosenberg, C., Field, M., Vianna-Morgante, A.M., Christie, L., Krepischi-Santos, A.C., Banna, L., Brereton, A.V., Hill, A., Bisgaard, A.M., Müller, I., Hultschig, C., Erdogan, F., Wieczorek, G., and Ropers, H.H. (2007). Array CGH identifies reciprocal 16p13.1 duplications and deletions that predispose to autism and/or mental retardation. Hum. Mutat. *28*, 674–682.

Vergnolle, M.A., and Taylor, S.S. (2007). Cenp-F links kinetochores to ndel1/nde1/lis1/dynein microtubule motor complexes. Curr. Biol. *17*, 1173–1179.

Vitale, I., Galluzzi, L., Castedo, M., and Kroemer, G. (2011). Mitotic catastrophe: a mechanism for avoiding genomic instability. Nat. Rev. Mol. Cell Biol. *12*, 385–392.

Wei, H., Zou, H., Sheikh, A.M., Malik, M., Dobkin, C., Brown, W.T., and Li, X. (2011). IL-6 is increased in the cerebellum of autistic brain and alters neural cell adhesion, migration and synaptic formation. J. Neuroinflammation *8*, 52.

Williams, N.M., Zaharieva, I., Martin, A., Langley, K., Mantripragada, K., Fossdal, R., Stefansson, H., Stefansson, K., Magnusson, P., Gudmundsson, O.O., Gustafsson, O., Holmans, P., Owen, M.J., O'Donovan, M., and Thapar, A. (2010). Rare chromosomal deletions and duplications in attention-deficit hyperactivity disorder: a genome-wide analysis. Lancet *376*, 1401–1408.

STAR★METHODS

KEY RESOURCES TABLE

REAGENT or RESOURCE	SOURCE	IDENTIFIER
Bacterial and virus strains		
Plasmid: pCas9	Addgene	Cat: 42876
Plasmid: pcs108-nde1 ORF	This paper	N/A
Chemicals, peptides, and recombinant proteins		
Minocycline	Beyotime	Cat: ST1528
Anti-dig-AP, Fab fragments	Roche	Cat: 11093274910
Dig RNA labeling mix	Roche	Cat: 11277073910
Paraformaldehyde	Solarbio	Cat: P1112
TB Green Premix Ex Taq	TaKaRa	Cat: RR820A
Trizol	Ambion	Cat: 15596-026
Paraffin	Solarbio	Cat: YA0012
Critical commercial assays		
AO staining kit	Solarbio	Cat:CA1143
HE staining kit	Solarbio	Cat: G1102-3
mMESSAGE mMACHINE SP6 kit	Ambion	Cat: AM1304
PrimeScript™ RT reagent kit	TaKaRa	Cat: RR047A
Quick spin columns	Roche	Cat: 11274015001
Deposited data		
SRA RNA-seq data	This paper	PRJNA776712
Experimental models: Organisms/strains		
TU strain	Our lab	N/A
Nde1-KO	This paper	N/A
Software and algorithms		
GraphPad prism	Prism	https://www.graphpad.com/scientific-software/prism
Adobe illustrator	Adobe	https://www.adobe.com/cn/products/illustrator.html
Zebralab software	ViewPoint Life Sciences	N/A
Oligonucleotides		
Primers for nde1 ORF amplification, see Table S2	This paper	N/A
Primers for qPCR, see Table S3	This paper	N/A

RESOURCE AVAILABILITY

Lead contact

Further information and requests about this study should be directed to and will be fulfilled by the lead contact, Qiang Li (liq@fudan.edu.cn).

Material availability

This study did not generate new unique reagents. All requests for resources and reagents should be directed to the lead contact and will be made available on request after completion of a Materials Transfer Agreement.

Data and code availability

Sequencing data reported in this paper has been deposited to SRA (PRJNA776712) and is publicly available.

This paper does not report original code.

Any additional information required to reanalyze the data reported in this paper is available from the lead contact upon request.

EXPERIMENT MODEL AND SUBJECT DETAILS

Animals

2- and 3-month-old Wild type (Tu strain), and nde1$^{-/-}$ zebrafish were raised in a circulating water system at a constant temperature of 28.5 °C, and 14/10 h light/dark cycle. Embryos were collected by natural spawning after 1 h and incubated for 7 days in blue water. Then, the larvae were fed in the circulating water system. All animal experiments were approved by the institutional animal care committee of Children's Hospital of Fudan University (Ethical approval number: 2013-098).

METHOD DETAILS

Synthesis of Digoxigenin-labeled RNA probe and whole mount *in* situ hybridization

Primers with homologous arm were designed based on zebrafish *nde1* ORF sequence (GenBank Accession No: NM_001030203.1) and sequence of plasmid pcs108 (our lab), primer sequence were shown in Table S2. *nde1* ORF was obtained by RT-PCR from cDNA libraries and then inserted into pcs108 through seamless clone follow protocols of One Step Cloning Kit (C112, Vazyme, China). Then Digoxigenin-labeled antisense RNA probes were transcribed with T7 RNA polymerase (Thermo, USA), in the presence of Digoxigenin dNTP mix (Roche, Switzerland) from the linearized plasmids. The newly synthesized RNA probes were then purified by Quick Spin Columns (Roche, Basel, Switzerland) and stored at −80°C.

Whole mount *in situ* hybridization was carried out as described in published paper (Thisse and Thisse, 2008). Imaging was performed using a Nikon MODEL C-DSS230 (DIC images).

Generation of *nde1*$^{-/-}$ zebrafish using CRISPR/Cas9

N20 sequence (5′-gatgagtcgagactatgagg-3′) were designed with ChopChop (http://chopchop.cbu.uib.no). 50 ng/μL of Cas9 RNA and 150 ng/μL of guide RNA were co-injected into one-cell Tu strain zebrafish embryos. The F1 progenies were screened out the germ line mutation with sequence analysis of the genomic DNA. The identified heterozygote mutant zebrafish were mated with a Tu zebrafish to purify background and produce F2 progenies. The F2 heterozygote progenies were self-crossed to produce F3 progenies. The nde1$^{-/-}$ zebrafish were screened from F3 progenies.

Acridine orange (AO) staining

The AO staining was performed to study the apoptosis of zebrafish embryos. Briefly, the embryos were washed with 1x AO stain buffer (Solarbio, CA1143) for 5 min at room temperature. Then, the embryos were stained with Acridine orange (2 mg L^{-1} in AO stain buffer) at 4°C for 30 min in the dark. After the staining, the embryos were washed 3 times with PBS for 5 min each time. Stained embryos were photographed under Fluorescence stereo microscope (Leica, MA205). Apoptosis is characterized by apoptotic bodies which were stained as bright green apoptotic bodies. Quantitative statistics of apoptotic bodies of nervous system were counted using a computer algorithm (ImageJ, National Institutes of Health, Bethesda, MD, USA). Counts were verified by manual counting.

Brain weighing

Brain tissues of 3 mpf zebrafish were collected in centrifuge tubes with 60 brains per tube and weighed, n = 5. Simple comparisons between *nde1*$^{+/+}$ and nde1$^{-/-}$ zebrafish were determined by Student's *t* test.

Paraffin sections

The intact brain tissues of 3mpf zebrafish were collected and fixed in 4% paraformaldehyde for 24 h at 4 °C. Fixed brain tissues were dehydrated with 50%, 70%, 80%, 90%, 95%, 100%, and 100% ethanol each for 7 min.

After dehydration, the samples were soaked in xylene I and xylene II each for 5-6 min. Then incubated in melted paraffin at 60°C for 1 h on an NHP-1 hot plate. The brain tissues were incubated 3 times in melted paraffin and cooled until paraffin were set. Finally, Embedded brain tissues were sliced with a paraffin slicer (Leica, RM2235) with 4 μm thickness.

Hematoxylin-eosin (HE) staining

Paraffin-embedded brain tissue sections were dewaxed in xylene, hydrated with an alcohol gradient and stained in hematoxylin solution for 1 min. The slices were then decolorized in acid alcohol (0.4% HCL in EtOH) for 30 s. After decolorized, the slices were washed in running tap water, and stained with eosin for 6 min. The slices were observed under microscope (Leica, MA205) after sealed with neutral resin seal.

Transcriptome resequencing analysis (RNA-seq)

Total RNA was extracted from 2 mpf brain of nde1 and nde1 zebrafish using TRIzol® Reagent according the manufacturer's instructions (Ambion). cDNA libraries were constructed according to the manufacturer's standard protocol (Illumina, Inc.). The Oligo (dT) isolated mRNA was fragmented, and cDNA was synthesized using the mRNA fragments as templates. Then the synthesized cDNA was subjected to end-repair, phosphorylation and 'A' base addition according to Illumina's library construction protocol. During the QC steps, the Agilent 2100 Bioanaylzer and ABI StepOnePlus Real-Time PCR System were used in quantification and qualification of the sample libraries. Then the libraries were sequenced using the Illumina HiSeq 4000 platform. We filtered low-quality, adaptor-polluted, and high content of unknown base (N) reads to get clean reads. Clean reads were mapped to zebrafish genome sequence (version: GRCz11) as reference, and the matching rate ranged from 90.3% to 91.54%.

To identify DEGs between two different samples, the expression level of each transcript was calculated according to the fragments per kilobase of exon per million mapped reads (FRKM) method. DEGs were detected via DESeq2 (parameters: Fold Change $\geq$2.00 and Adjusted p $\leq$ 0.05). GO functional enrichment and KEGG pathway analysis were carried out by Goatools and KOBAS. (parameters: Bonferroni-corrected P-value $\leq$0.05).

RNA isolation, real-time PCR (qPCR)

Total RNA was extracted from whole embryos (30-50 embryos per sample) or adult zebrafish brain tissues (5-6 brains per sample) using TRIzol reagent (Ambion, USA). A PrimeScript™ RT Reagent Kit (RR047A, TaKaRa, Japan) was used to synthesize complementary deoxyribonucleic acid (cDNA) from 1 μg of total RNA stocks according to the manufacturer's protocol. Real-time PCR was performed using TB Green Premix Ex Taq (RR820A, TaKaRa, Japan) on a LightCycler® 480 apparatus (Roche, Germany), according to the manufacturers' instructions. The delta delta CT method was used to calculate the expression levels. The primer sequences used in Real-time PCR are shown in Table S3.

Capped *nde1* mRNA synthesis

Capped *nde1* mRNA was synthesized *in vitro* from linearized pcs108-*nde1* ORF using the mMESSAGE mMACHINE SP6 Kit (Ambion, USA). Before injection, mRNA was purified by Quick Spin Columns (Roche, Switzerland) and diluted in RNase-free water.

Microinjection

All the samples were injected into the blastodisc at the 1 to 2-cell stage.

Behavioral experiments

All behavioral tests were performed in our behavioral assessment room, with ambient temperature at 28.5 °C. Behavioral experiments were carried out between 9:00 am and 4:00 pm. Zebrafish's behaviors were quantified by the Zebralab software (ViewPoint Life Sciences, Lissieu, Calvados, Lower Normandy Region, France). Detailed procedures of each test are summarized as follows.

Larval activity

The behavior tests of 5dpf larvae were carried out in 24-well plates (the inner diameter of each well was 18 mm) (Ji et al., 2017; Li et al., 2015). Then put the 24-well plates into a Zebrabox apparatus (ViewPoint Life Sciences, Lissieu, Calvados, Lower Normandy Region, France) to record 75 min video of zebrafish

larvae activities. The zebrafish larvae were first given a 55 min continuous illumination at 110 Lx, followed by two light/dark cycles (5 min illumination followed by 5 min dark). The Zebralab software was used to quantify the zebrafish larvae locomotor activities with recorded videos. The videos were taken at the rate of 25 frames per second, and were pooled into 1 min time bins. The distance swum by the larvae in the whole well was extracted to analyze locomotor activities.

Open-field locomotor activity test

For open-field test, fish was tested at 2 mpf and 3 mpf. Each tank was 30 × 30 × 30 cm and filled with 5 cm-height water from circulating water system. The walls were made of opaque white partitions, and a camera was suspended above the tank. Each fish was put into the tank alone, and was allowed to swim freely. Testing sessions was recorded for 30 min. Afterwards, recordings were analyzed with our tracking software, including locomotor activities (distance traveled) and repetitive behavior. Repetitive behavior includes back and forth, small circles, and big circles. Definition of the back and forth is that the zebrafish repeatedly swim back and forth on one side of the tank at least once. The small circles defined that the zebrafish swims a circle from the beginning to the end less than 30 mm, and the swimming time is greater than 5s. The large circles mean that the zebrafish swim counterclockwise or clockwise along the edge of the tank for more than one circle. All data were analyzed after video recording for 10 min.

Shoaling test

Six 2 mpf or 3 mpf zebrafish of the same sex were placed in a tank, and allowed to swim freely. Zebrafish were recorded for 30 min (Liu et al., 2018). The shoaling assessment was performed by calculating the average distance between any two zebrafish, and indicated the social behaviors of zebrafish. All data were analyzed after video recording for 10 min.

Social preference test

Social preference testing was performed in a transparent mating tank (inner dimensions 21 × 10 × 7.5 cm). A transparent separator was used to separate the tank into two same size halves. The tested zebrafish (2mpf or 3mpf) were put on one side of the tank with a group of six conspecific zebrafish on another side (Figure 4C). Their behavior was recorded for 30 min. For the data analysis, the time ratio and distance ratio that zebrafish spent in the zone nearest to their companion (social zone) were calculated. All data were analyzed after video recording for 10 min.

Kin preference test

The mating tank used in the kin preference test was the same as those in the social preference test. Two transparent separators divided the tank into three compartments. The tested zebrafish (3 mpf) were put on Middle compartment of the tank, with three kin zebrafish placed on the left and three non-kin (red color) zebrafish placed on the right (Figure 4E). Their behavior was recorded for 30 min the time ratio and distance ratio that zebrafish spent in the kin sector or non-kin sector were calculated as represented kin preference. All data were analyzed after video recording for 10 min.

Minocycline treatment

3 mpf WT and *nde1* deficiency zebrafish were treated with 10 μM minocycline for 4 weeks. Fresh minocycline water was replaced every day. Zebrafish were placed in a low light environment for minocycline is easily decomposed by light.

QUANTIFICATION AND STATISTICAL ANALYSIS

Statistical analysis and mapping in this study were performed using GraphPad Prism 6.0. Data are shown as mean ± SEM. Simple comparisons between $nde1^{+/+}$ and $nde1^{-/-}$ zebrafish were determined by Student's *t* test or Mann-Whitney test. Values at *$p < 0.05$ were considered that there is a statistically significant.